Jurnal Rekayasa Mesin
p-ISSN: 1411-6863, e-ISSN: 2540-7678
Vol.21, No.1, April **2026**, p. 23-30

Characterization of the Material Produce by Wire Arc Additive Manufacturing GTAW Material AISI 308L

Edi Sarwono*, Dito Ardiyansyah
Department Mechanical Engineering, Sekolah Tinggi Teknologi "Warga" Surakarta,
Jl. Raya Solo - Baki No.Km 2, Kwarasan, Kec. Grogol, Kabupaten Sukoharjo, Jawa Tengah
*E-mail: edi@sttw.ac.id

Submitted: 30-09-2025; Accepted: 21-04-2026; Published: 30-04-2026

Abstract

This study examines the microstructural evolution & mechanical performance of AISI 308L stainless steel produced by Wire Arc Additive Manufacturing (WAAM) using the Gas Tungsten Arc Welding (GTAW) process. Specimens were sectioned into bottom, middle, & top regions to assess the effects of thermal cycling on hardness and tensile properties. Distinct microstructural and mechanical variations were observed along the manufacturing height. The bottom region, subjected to repeated reheating, exhibits coarse columnar & dendritic grains with a high δ-ferrite content, resulting in the lowest tensile strength (540 MPa) & hardness (230-255 HV), but the highest ductility (45% elongation). The middle region, influenced by in-situ thermal treatment, develops finer equiaxed grains and reduces porosity, resulting in increased tensile strength (547 MPa) & hardness (230-255 HV) with moderate ductility (35-38%). The top region, characterized by rapid cooling, forms fine equiaxed grains with minimal δ-ferrite, resulting in the highest hardness (265 HV) & tensile strength (546 MPa), albeit with reduced ductility (28-30%). These results extend previous investigations by quantitatively explaining the trade-off between strength & toughness across the WAAM layer. These findings confirm that grain refinement increases hardness and strength through grain boundary strengthening, while coarser grains increase ductility. Overall, this study underscores the important role of thermal history in tailoring mechanical performance & challenges the oversimplified notion that finer grains are always advantageous.

Keywords: AISI 308L; Additive Manufacturing; GTAW; Microstructure; WAAM

Abstrak

Studi ini meneliti evolusi mikrostruktur dan kinerja mekanik baja tahan karat AISI 308L yang diproduksi dengan Wire Arc Additive Manufacturing (WAAM) menggunakan proses Gas Tungsten Arc Welding (GTAW). Spesimen dipotong menjadi wilayah bawah, tengah, & atas untuk menilai efek siklus termal pada kekerasan dan sifat tarik. Variasi mikrostruktur dan mekanik yang berbeda diamati sepanjang ketinggian manufaktur. Daerah bawah, yang mengalami pemanasan ulang berulang, menunjukkan butiran kolumnar dan dendritik kasar dengan kandungan δ-ferit yang tinggi, menghasilkan kekuatan tarik terendah (540 MPa) dan kekerasan (230-255 HV), tetapi daktilitas tertinggi (45% perpanjangan). Daerah tengah, yang dipengaruhi oleh perlakuan termal in-situ, mengembangkan butiran equiaxed yang lebih halus dan mengurangi porositas, menghasilkan peningkatan kekuatan tarik (547 MPa) dan kekerasan (230-255 HV) dengan daktilitas sedang (35-38%). Daerah atas, yang ditandai dengan pendinginan cepat, membentuk butiran equiaxed halus dengan δ-ferit minimal, menghasilkan kekerasan tertinggi (265 HV) & kekuatan tarik (546 MPa), meskipun dengan daktilitas yang berkurang (28-30%). Hasil ini memperluas penelitian sebelumnya dengan menjelaskan secara kuantitatif pertukaran antara kekuatan dan ketangguhan di seluruh lapisan WAAM. Temuan ini menegaskan bahwa penghalusan butir meningkatkan kekerasan & kekuatan melalui penguatan batas butir, sementara butir yang lebih kasar meningkatkan daktilitas. Secara keseluruhan, penelitian ini menggarisbawahi peran penting riwayat termal dalam menyesuaikan kinerja mekanik & menantang anggapan yang terlalu disederhanakan bahwa butir yang lebih halus selalu menguntungkan.

Kata kunci: AISI 308L; *Additive Manufacturing*; GTAW; Struktur mikro; WAAM

1. Introduction

The rapid development of additive manufacturing (AM) technology has significantly transformed industrial component production by enabling complex geometries, reducing material waste, & increasing efficiency [1]. Among various AM techniques, Wire Arc Additive Manufacturing (WAAM) has attracted considerable attention due to its ability to fabricate large-scale metal components using arc welding heat sources & metal wire as raw materials [2]. Compared with powder-based AM methods such as Selective Laser Melting (SLM) or Electron Beam Melting (EBM), WAAM

offers distinct advantages including lower production costs, higher deposition rates, & scalability for industrial applications [3].

AISI 308L stainless steel, an austenitic alloy, is widely used in the food industry [4], chemical processing, healthcare, and marine environments due to its excellent corrosion resistance, high ductility, and thermal stability [5–7]. Despite these favorable properties, AISI 308L components fabricated with WAAM still face critical challenges. Reported issues include microstructural heterogeneity caused by uneven cooling rates, variations in mechanical performance, and susceptibility to porosity and thermal cracking [8–10].

Previous studies on WAAM have primarily focused on optimizing process parameters such as welding current, voltage [11], wire feed speed, & deposition path strategy [12]. Although these investigations have advanced process control, comprehensive characterization of AISI 308L fabricated with WAAM particularly in terms of microstructure, hardness, toughness, & tensile properties remains limited [13]. This gap highlights the need for deeper insight into the correlation between thermal history, grain morphology, & mechanical performance to ensure the reliability of WAAM components [14].

Therefore, this study aims to investigate the microstructural evolution and mechanical properties of AISI 308L stainless steel fabricated with WAAM using the Gas Tungsten Arc Welding (GTAW) method. This research specifically addresses how repeated thermal cycling during deposition affects grain structure, hardness, and tensile behavior across various manufacturing regions. By bridging this knowledge gap, this study seeks to provide a more comprehensive understanding of the interplay between strength, ductility, and toughness in WAAM-fabricated stainless steels, thereby contributing to process optimization and improved industrial applications.

2. Material and Method

This chapter contains important research data, equipment used and research location. The research method used is explained briefly (can be made in the form of a flow chart). New or modified methods should be explained in detail.

2.1. Specimen manufacture

The specimen fabrication process was carried out using the Wire Arc Additive Manufacturing Gas Tungsten Arc Welding (WAAM-GTAW) method, as shown in Figure 1, where the torch movement was controlled by a simple automatic system to maintain a constant motion. ER308L metal wire with a 1 mm diameter, produced by Kiswell Ltd, was selected as the deposition material based on the desired material composition for the specimen. The WAAM-GTAW parameters included a welding current of 120 A, a voltage of 32.6 V, argon shielding gas at 15 L/min, and a welding speed of 145 mm/s.

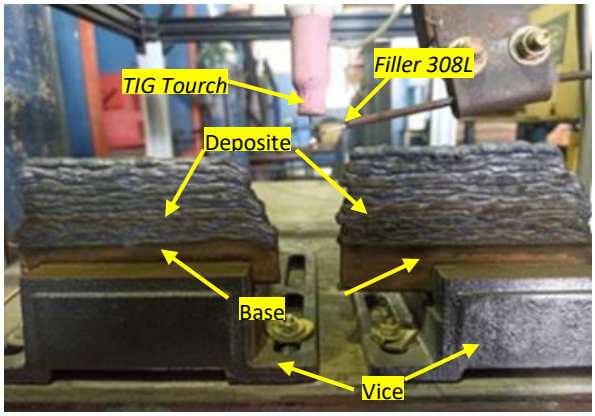

Figure 1. AISI 308L deposite manufacturing WAAM-GTAW process

The fabrication process continued until a deposit height of 75 mm above the substrate surface was achieved. After welding, the resulting specimen was cooled at room temperature. Following fabrication, the deposit was cut as shown in Figure 2 using wire cutting to avoid excessive heat, resulting in the specimen shown in Figure 3a. The specimen dimension according ASTM E8 (subsize specimen) explain at Figure 3b was divided into three regions: the bottom specimen (Bottom area), the middle specimen (Middle area), and the top specimen (Top area).

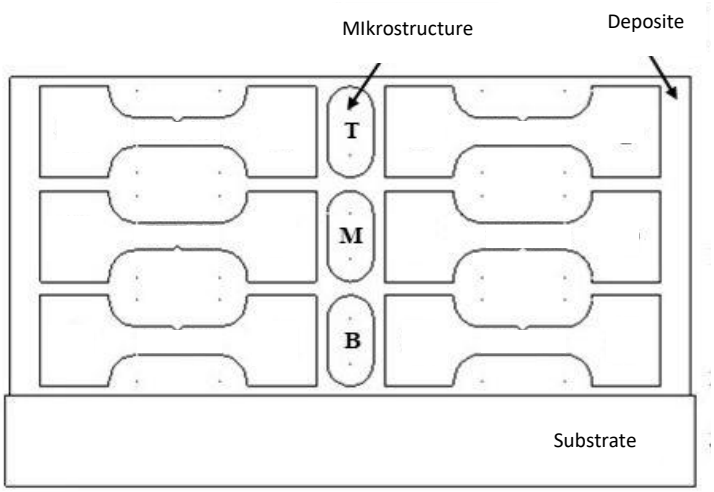

Figure 2. Sketch of wire cut sectioning of the deposit into specimen

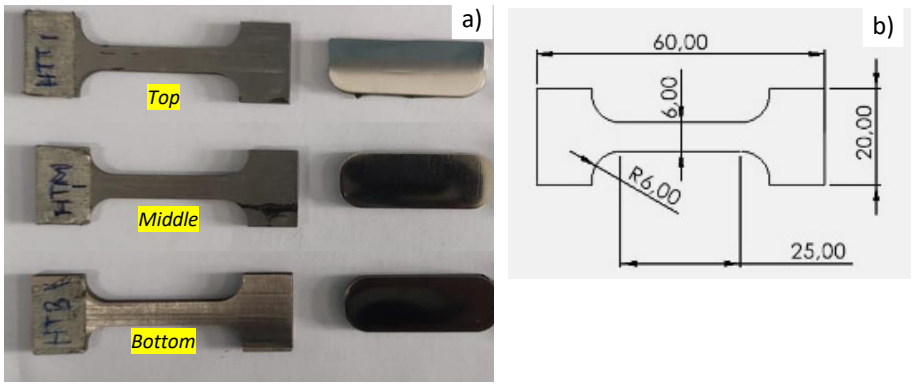

Figure 3. Result of deposit cutting (a) and specimen dimensions in mm (b)

2.2. Specimen characterization

Microstructure observation was conducted using a microscope to examine the structure of the tested material. Prior to this, surface treatment was performed using sandpaper with grades 100-2000, followed by polishing with alumina paste. An etching solution consisting of 10 ml HCl, 10 ml HNO3, and 10 ml distilled water was used to reveal the grain boundaries, making the microstructure of the tested material more visible. The microscope used was an OLYMPUS brand, with magnification ranging from 50x to 1000x.

Tensile strength testing was conducted using a TIME WEW-600D Universal Tensile Testing Machine, with a maximum testing capacity of 600 kN, equipped with hydraulic clamps to hold the test specimen. This machine was used to measure the maximum tensile strength and yield stress of the specimen. Additionally, the machine is equipped with software that allows real-time reading of stress-strain graphs during the test.

Hardness testing was performed using the Vickers hardness testing ASTM E384 method. The hardness testing device used in this study was a TIME DHV-1000z. A load of 9.8 N was applied with a dwell time of 15 seconds. The testing

was conducted along the specimen from the bottom (Bottom) to the top (Top) regions sequentially to assess the hardness distribution, with a spacing of 0.5 mm, as shown in Figure 4.

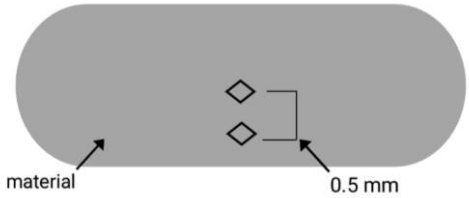

Figure 4. Hardness position and target point test

3. Results and Discussion

3.1. Results

The results of the microstructure testing reveal the presence of ferrite (dark) and austenite (white/bright), which are characteristic features of austenitic steel. Microstructure testing at 200x magnification on the Top area is shown in Figure 4. The image results indicate that the ferrite formed exhibits a lathy mode. Figure 5 shows the ferrite formed in the middle region, which also exhibits a lathy mode, but is more dominant than in the Top specimen.

The tensile test results are summarized in Table 1. The stress-strain graph from the tensile test, shown in Figure 7, facilitates the analysis of the stress-strain behavior of the specimen. The tensile strength results show slight differences. The highest yield strength value is observed in the Bottom specimen, while the Top and Middle specimens have the same yield strength value. The Bottom specimen exhibits better elongation compared to the Top and Middle specimens.

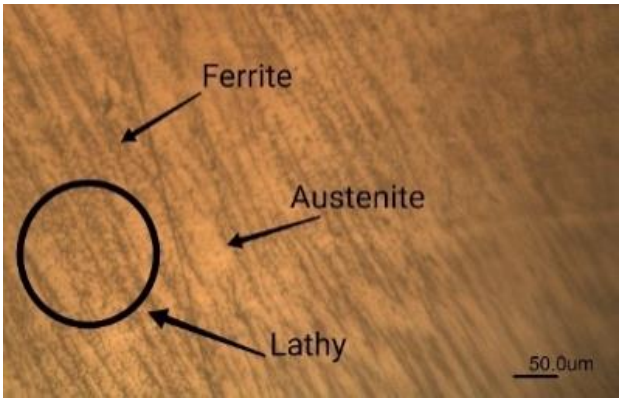

Figure 5. Top specimen microstructure

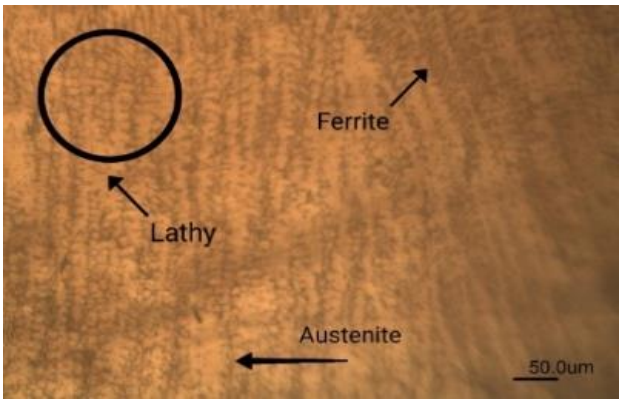

Figure 6. Middle specimen microstructure

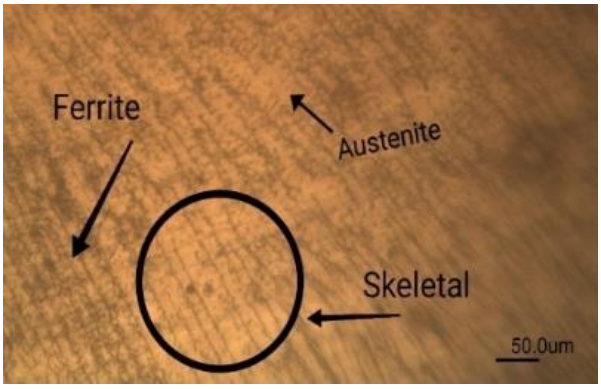

Figure 7. Bottom specimen microstructure

The studies by Li et al. (5) and Le et al. (6) show similarities in the Bottom specimen region, where repeated thermal cycles occur due to additional heating from each new layer, resulting in the formation of columnar grains that extend in the direction of the thermal gradient, with a coarse dendritic structure due to the slow initial cooling rate. In this area, many skeletal delta-ferrite structures are present within the austenitic matrix. The Middle specimen undergoes repeated heating, creating natural heat treatment, which results in finer grains with a predominance of equiaxial and more homogeneous mixed equiaxial dendritic structures, accompanied by evenly distributed lathy delta ferrite. Meanwhile, the Top specimen, which experiences only one heating cycle and rapid cooling, forms fine equiaxial grains with fine dendrites and the least amount of delta ferrite, generally in the form of thin lathy structures.

The tensile test results are summarized in Table 1. The stress-strain graph from the tensile test, shown in Figure 8, facilitates the analysis of the stress-strain behavior of the specimen. The tensile strength results show slight differences. The highest yield strength value is observed in the Bottom specimen, while the Top and Middle specimens have the same yield strength value. The Bottom specimen exhibits better elongation compared to both the Top and Middle specimens.

Table 1. Tensile strength test result specimen WAAM-GTAW AISI 308L

Specimen	Tensile strength (MPa)	Yield strength (MPa)
Top	545.94	372
Middle	547.17	372
Bottom	540.35	395

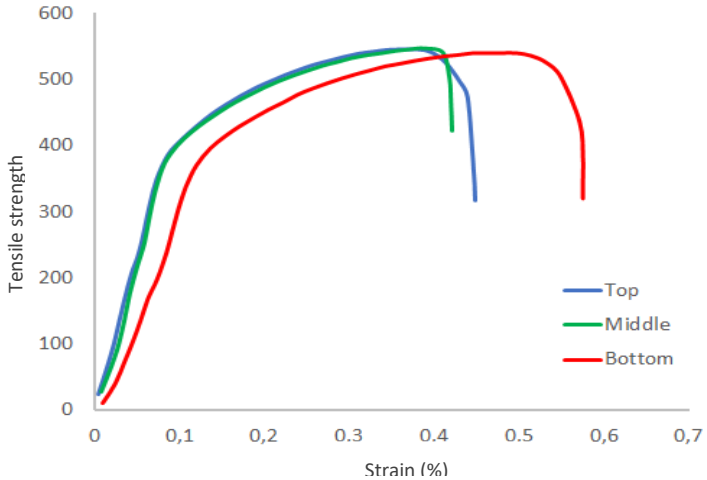

Figure 8. Tensile strength test result graph

The tensile test results in Figure 9 show the distribution of hardness values from the bottom to the top region. The highest hardness of 267.2 HV is found at the bottom area. The Middle region has an average hardness ranging from 254.8 HV to 229.6 HV. The top region has the highest hardness of 265.2 HV at point 25.

Figure 9. Hardness vickers test result

3.2. Discussion

The WAAM-GTAW process applied to AISI 308L stainless steel produced distinct microstructural variations across the deposited layers, strongly influenced by thermal cycling and cooling rates. In the bottom region, repeated reheating from subsequent layers promoted the formation of columnar grains aligned with the thermal gradient and a coarse dendritic structure due to the slow initial cooling rate. This observation is consistent with Chamim et al. [15], who reported similar grain morphologies under repeated thermal exposure. The presence of skeletal delta-ferrite within the austenitic matrix was frequently observed, which mitigates hot cracking susceptibility. However, the coarse grain morphology correlates with reduced tensile strength despite higher fracture strain, confirming Andrade et al. [4] that coarse grains enhance toughness but compromise strength. In the middle region, repeated heating acted as a natural heat treatment zone, refining the microstructure into predominantly equiaxed grains with a more homogeneous dendritic distribution. This refinement resulted in improved mechanical properties, with reduced porosity and enhanced grain uniformity. Such microstructural stabilization aligns with Li et al. [5] and Le et al. [6], who demonstrated that reheating in WAAM stainless steels promotes recrystallization and porosity reduction. The top region, subjected to only a single thermal cycle, experienced rapid cooling that produced fine equiaxed grains with fine dendrites and a lower fraction of delta-ferrite. This microstructural refinement yielded the highest hardness and tensile strength, consistent with Zou et al. [16], who emphasized that rapid cooling enhances grain boundary strengthening but simultaneously reduces ductility.

Hardness testing (Figure 9) revealed a gradient across the layers. The bottom region exhibited fluctuating hardness values, with the lowest average (229–254 HV) and a decreasing trend toward the middle region. This correlates with tensile testing (Figure 8), where the bottom layer showed the lowest tensile strength (540 MPa) but the highest yield strength (395 MPa) and fracture strain (elongation up to 45%), indicating ductility associated with coarse grains. The middle region demonstrated stabilized hardness values (230-255 HV) and improved tensile strength (547 MPa), with yield strength at 372 MPa and fracture strain reduced to 35%. This balance between strength and ductility reflects the homogenized equiaxed grain structure. The top region exhibited the highest hardness (265 HV) and tensile strength (546 MPa), but fracture strain decreased to 28-30%, indicating reduced ductility. Compared with the bottom region, the top region demonstrated 10% increase in hardness and 12% increase in tensile strength, but 35% reduction in ductility, highlighting the trade-off between strength and toughness in WAAM-fabricated stainless steels.

These findings critically extend prior work. Chamim et al. [15] and Andrade et al. [4] emphasized the role of thermal cycling and grain morphology in mechanical performance, but lacked quantitative evidence across multilayer WAAM structures. The present results reconcile their observations by demonstrating that coarse grains indeed enhance ductility but reduce strength, while fine grains maximize strength at the expense of ductility. Vora et al. [17] confirmed grain boundary strengthening mechanisms, and the present study extends this by quantifying the relationship between cooling rate, grain size, and mechanical properties.

Furthermore, the reduction in porosity observed in the middle region strengthens the conclusions of Kumar et al. [14] and Senthil et al. [12], who reported recrystallization driven homogenization in WAAM stainless steels. The present study corrects the oversimplified assumption that finer grains are universally superior, instead demonstrating that layer position and thermal history dictate the balance between strength, hardness, and ductility.

4. Conclusion

This study demonstrates that the thermal history across the deposition layer governs the microstructural evolution and mechanical performance of AISI 308L stainless steel fabricated with WAAM. The bottom region, which is repeatedly heated, develops coarse columnar grains with higher δ-ferrite, resulting in lower strength and hardness but superior ductility. The middle region benefits from in-situ heat treatment, resulting in finer equiaxed grains and reduced porosity, which balances strength, hardness, and ductility. The top region, which is rapidly cooled, forms fine equiaxed grains with minimal δ-ferrite, resulting in the highest hardness and strength but reduced ductility. These findings highlight the trade-off between grain refinement and toughness, suggesting that finer grains are not always advantageous. Overall, these results emphasize the importance of process parameter optimization and thermal management in WAAM to optimize mechanical properties to specific service applications.

Acknowledgement

We would like to thank the Welding Laboratory team for providing facilities and access for this research.

References

[1] Zhou L, Miller J, Vezza J, Mayster M, Raffay M, Justice Q, et al. Additive Manufacturing: A Comprehensive Review. Vol. 24, Sensors. Multidisciplinary Digital Publishing Institute (MDPI); 2024.

[2] Solomon IJ, Srinivas J, Leon SJ, Ramesh A, Rohith IJ, Senthil TS. Mechanical and microstructural investigation of multi-layered Inconel 825 wall fabricated using CMT-based WAAM. Journal of Alloys and Metallurgical Systems. 2024 Dec 1;8.

[3] Williams SW, Martina F, Addison AC, Ding J, Pardal G, Colegrove P. Wire + Arc Additive Manufacturing. Materials Science and Technology [Internet]. 2016 May 1;32(7):641–7. Available from: https://journals.sagepub.com/doi/10.1179/1743284715Y.0000000073

[4] Andrade DG, Tankova T, Zhu C, Branco R, da Silva LS, Rodrigues DM. Mechanical properties of 3D printed CMT-WAAM 316 LSi stainless steel walls. J Constr Steel Res. 2024 Apr 1;215.

[5] Li M, Lu T, Dai J, Jia X, Gu X, Dai T. Microstructure and mechanical properties of 308L stainless steel fabricated by laminar plasma additive manufacturing. Materials Science and Engineering A [Internet]. 2020;770(October 2019):138523. Available from: https://doi.org/10.1016/j.msea.2019.138523

[6] Le VT, Mai DS, Doan TK, Paris H. Wire and arc additive manufacturing of 308L stainless steel components: Optimization of processing parameters and material properties. Engineering Science and Technology, an International Journal [Internet]. 2021;24(4):1015–26. Available from: https://doi.org/10.1016/j.jestch.2021.01.009

[7] Hsu CH, Chen TC, Huang RT, Tsay LW. Stress corrosion cracking susceptibility of 304L Substrate and 308L weld metal exposed to a salt spray. Materials. 2017;10(2):1–14.

[8] Ali MH, Han YS. Effect of phase transformations on scanning strategy in waam fabrication. Materials. 2021 Dec 1;14(24).

[9] Oktadinata H, Martijanti M, Ndaruhadi PYMW, Alsayed EA. Study of Sensitization in Gas Tungsten Arc Welded 304 Stainless Steel Joints Using 308L Filler Metal. Construction Technologies and Architecture [Internet]. 2024;11:3–9. Available from: https://www.scientific.net/CTA.11.3

[10] Singh S, Ramakrishna S, Singh R. Material issues in additive manufacturing: A review. J Manuf Process [Internet]. 2017; 25(January): 185–200. Available from: http://dx.doi.org/10.1016/j.jmapro.2016.11.006

[11] Koli Y, Aravindan S, Rao P V. Influence of heat input on the evolution of δ-ferrite grain morphology of SS308L fabricated using WAAM-CMT. Mater Charact [Internet]. 2022;194(May):112363. Available from: https://doi.org/10.1016/j.matchar.2022.112363

[12] Senthil TS, Babu SR, Puviyarasan M, Balachandar VS. Experimental investigations on the multi-layered SS316L wall fabricated by CMT-based WAAM: Mechanical and microstructural studies. Journal of Alloys and Metallurgical Systems. 2023 Jun 1;2.

[13] Singh S, Sharma SK, Rathod DW. A review on process planning strategies and challenges of WAAM. Mater Today Proc [Internet]. 2020;47(xxxx):6564–75. Available from: https://doi.org/10.1016/j.matpr.2021.02.632

[14] Kumar V, Mandal A. A critical investigation of the anisotropic behavior in the WAAM-fabricated structure. Rapid Prototyp J [Internet]. 2024 Jan 1;30(5):1023–45. Available from: https://doi.org/10.1108/RPJ-01-2023-0005

[15] Chamim M, Darmadi DB, Purnowidodo A, Widodo TD, Ismail Z. Influence of the welding thermal cycle on δ-ferrite evolution in the first layer of Austenitic Stainless Steel (ASS) 308L produced by WAAM-GTAW. Case Studies in Thermal Engineering [Internet]. 2024;105489. Available from: https://www.sciencedirect.com/science/article/pii/S2214157X2401520X

[16] Zou X, Niu B, Pan L, Yi J. Wire + Arc Additive Manufacturing and Heat Treatment of Super Martensitic Stainless Steel with a Refined Microstructure and Excellent Mechanical Properties. Materials. 2022 Apr 1;15(7).

[17] Vora J, Parmar H, Chaudhari R, Khanna S, Doshi M, Patel V. Experimental investigations on mechanical properties of multi-layered structure fabricated by GMAW-based WAAM of SS316L. Journal of Materials Research and Technology. 2022 Sep 1;20:2748–57.